

Confinement in the Coulomb Gauge Model

Th. Wilke and S. P. Klevansky

Institut für Theoretische Physik,

Philosophenweg 16 u. 19, D-69120 Heidelberg, Germany

Abstract

The Coulomb gauge model of QCD is studied with the introduction of a confining potential into the scalar part of the vector potential. Using a Green function formalism, we derive the self-energy for this model, which has both scalar and vector parts, $\Sigma^S(p)$ and $\Sigma^V(p)$. A rotation of these variables leads to the so-called gap and energy equations. We then analyse the divergence structure of these equations. As this depends explicitly on the form of potential, we give as examples both the linear plus Coulomb and quadratically confining potentials. The nature of the confining single particle Green function is investigated, and shown to be divergent due to the infrared singularities caused by the confining potential. Solutions to the gap equation for the simpler case of quadratic confinement are found both semi-analytically and numerically. At finite temperatures, the coupled set of equations are solved numerically in two decoupling approximations. Although chiral symmetry is found only to be exactly restored as $T \rightarrow \infty$, the chiral condensate displays a steep drop over a somewhat small temperature range.

I. INTRODUCTION

From a phenomenological and experimental viewpoint, two aspects of quantum chromodynamics (QCD) are believed to be fundamental, (a) that chiral symmetry is spontaneously broken in the ground state and (b) that partons are confined. Both chiral symmetry and the phenomenon of confinement underly a common speculation, viz. that each is believed to give rise to a phase transition at a characteristic temperature or density $T_\chi(T_c)$ and $\rho_\chi(\rho_c)$ respectively. As a side remark, one may note that these two phase transitions have a very different character - the chiral order parameter is zero in the ordered phase, and non-zero in the broken phase, in character with the notions of condensed matter physics, while the confinement transition has an inverted structure: the non-zero value of the order parameter, or Polyakov line in this case, usually characterizes the deconfined or ordered phase. The current belief, stemming from lattice gauge simulations, is that, for QCD including quarks, the critical temperatures coincide [1]. This feature is not understood on a firm basis, and is merely an empirical observation.

Phenomenological studies over the last decade have predominantly investigated the chiral symmetry aspect of QCD. For example, the Nambu–Jona-Lasinio (NJL) model [2,3] has enjoyed tremendous success, due to its mathematical tractability and ease of use. Calculations of the low-energy mesonic and baryonic sectors demonstrate the well-known fact that chiral symmetry is broken at $T = 0$ in nature. From a theoretical point of view, one can study the model at finite temperatures and densities, but it is clear that the thermodynamical potential and associated bulk quantities will be dominated by inadmissible quark degrees of freedom in an intermediate temperature region where they should not exist at all [4]. One conceivable method of removing this problem is to start with a confining model in the first place. This in itself presents many new difficulties that are not inherent in the non-confining NJL model. The fundamental theoretical questions that must be answered are (i) what is the analytic structure of a Green function that describes a confined particle [5], and (ii) what is the role and connection of chiral symmetry, if any, with confinement and the deconfining transition. In addition, such a model must be required to reproduce the excellent agreement of non-confining chiral models with experiment, which in itself, is no mean task due to the added complexity. Yet a further complication

is that the nature of an effective deconfinement potential is not precisely known. Bag model calculations suggest that confinement should be introduced in a scalar potential [6], while Coulomb gauge QCD naturally favors vector confinement. More detailed study is required to clarify this issue fully. Finally, even the understanding of these features still leaves the question open as to how the model should *deconfine* dynamically.

Several authors have attempted to address the problem that is associated with (i) above, i.e. of the analytic structure of a Green function for a confined quark [5,7]. Because of the various problems that are connected with these attempts (e.g. non-causality in the case of [8], and so on), this question is still not completely settled. In this paper, we do not make any assumptions about the form of the single quark Green function. Rather, we choose to study a model Lagrangian that contains a confining potential, and directly compute the Green function, assuming that it satisfies a Dyson-like equation. The feature of confinement should reflect itself *automatically* in the Green function and our task is to make this evident. Choosing a form for a confining interaction is not unique however. We have chosen to study the Coulomb gauge model [9] that employs vector confinement as a starting point, simply because this model has been studied by several authors previously [9–17]. As such, this work is not entirely new: however, it unites previously unrelated work, and presents this model in a conceptual fashion that is different from most interpretations. Differences in the existing literature are clarified. The temperature dependence in this model is also examined. Here there are two different approaches that are possible, either that of Green functions in the real or imaginary time formalism, see for example [12], or via a variational principle that is applied to the free energy [17]. We use the former approach - one can explicitly see that it leads to equations that are entirely equivalent to those obtained in the latter approach. Here there has been some conflict in the literature. The gap equation that we have derived in this fashion corresponds to that derived by Ref. [17] on varying the free energy, but is in conflict with that of Ref. [11] who disregard the temperature dependence of the quasiparticle energy, as well as that of Ref. [13] who simply write down a different gap equation. Further conflict arises also in the interpretation of the quasiparticle energy. In this paper, we utilize the knowledge gained from the invariance structure at zero temperature, $T = 0$, and implement a similar procedure at finite temperatures. Central to our approach is

the appearance of physical quasiparticle energies that are temperature dependent, as is the case in the BCS theory of superconductivity for low temperatures. It is essentially this temperature dependence which is capable of driving a phase transition, and which is studied here. This is in apposition to models that introduce an effective temperature dependence in the coupling strength, see, for example Ref. [13], which is difficult to deal with consistently from a thermodynamical point of view. In the case studied here, we keep the coupling constant fixed and examine the consequences of the temperature dependent quasiparticle energies. Numerical solutions are given for the coupled set of equations that form the gap equation in this case. It is interesting to note that although in part only approximate solutions can be given, the model dependence of $\langle\bar{\psi}\psi\rangle$ closely resembles that of the lattice simulations [20]. Chiral symmetry, is however, not restored exactly. It would thus be of great interest in the future to have lattice simulations that could quantify the range of the drop in temperature of the chiral order parameter.

Finally, one should note that the Coulomb gauge model, while appearing intuitively physical, is by definition no longer manifestly gauge covariant, as is the non-confining NJL model. However, since any potential introduced into the NJL model would also be expected to be instantaneous, this covariance is unavoidably lost. Thus a study of the Coulomb gauge model should provide many features that should be generic to four-fermion interactions and should be similarly handled in, for example, an extended NJL model that includes confinement.

We point out that currently there has been a surge of interest in the problem of confinement. For different approaches, we refer the interested reader also to the works of Refs. [18,19,21–23]. This list of references is, however, not exhaustive.

This paper is organized as follows. In Section II, the general formalism is developed for $T = 0$ for an arbitrary potential. The form of the single particle propagator is given and the distinction between observables and non-observables is made according to the conditions of ultraviolet renormalizability as well as infrared finiteness. These divergences are discussed for two particular types of potentials, the Coulomb plus linear rising potential and the quadratically confining potential. In Section III, the solutions of the gap equation for a quadratically confining potential are discussed in this framework. In Section IV, the extension to finite temperatures is given, and numerical solutions for the condensate and dynamical mass is given. We summarize

and conclude in Section V.

II. FORMALISM FOR $T = 0$

A. Self-consistent self-energy

Our starting point is the Coulomb gauge QCD Hamiltonian, given by

$$\begin{aligned}\hat{H} &= \hat{H}_0 + \hat{H}_1 \\ &= \int d^3x \hat{\psi}^\dagger(\vec{x}) (-i\vec{\alpha} \cdot \vec{\nabla}) \hat{\psi}(\vec{x}) \\ &\quad + \sum_{a=1}^8 \int d^3x d^3y \hat{\psi}^\dagger(\vec{x}) \frac{\lambda_a}{2} \hat{\psi}(\vec{x}) V(\vec{x} - \vec{y}) \hat{\psi}^\dagger(\vec{y}) \frac{\lambda_a}{2} \hat{\psi}(\vec{y}),\end{aligned}\tag{2.1}$$

where λ_a are the standard Gell-Mann matrices, and $V(\vec{x})$ is an arbitrary potential at this point, and which will be considered to be confining. No current quark masses are considered.

In general, the self-consistent self-energy $\Sigma(p)$ associated with the interaction is a function of momentum. Under the assumption that the quark propagator is diagonal and independent of color, $S(k)_{c,c'} = S(k)\delta_{c,c'}$, one has the mathematical consequence that the Hartree term vanishes. Thus the leading non-vanishing contribution to the self-energy, calculated to lowest order in the interaction strength follows from the Fock diagram that is depicted in Fig.1. One finds

$$\Sigma(\vec{p}) = i \sum_{a=1}^8 \int \frac{d^4k}{(2\pi)^4} V(\vec{p} - \vec{k}) \gamma_0 \frac{\lambda_a}{2} S(k) \gamma_0 \frac{\lambda_a}{2},\tag{2.2}$$

where $S(k)$ is the self-consistently evaluated one particle fermion Green function, of form

$$S(p)^{-1} = \not{p} - \Sigma(p).\tag{2.3}$$

Note that this structure is particular to this form of the interaction, and, as such, may not be taken as being generic to confinement *per se*. Lorentz symmetry and invariance under a parity transformation enable one to decompose $\Sigma(p)$ into a scalar and vector term,

$$\Sigma(\vec{p}) = \Sigma^S(|\vec{p}|) + \vec{\gamma} \cdot \hat{p} \Sigma^V(|\vec{p}|),\tag{2.4}$$

where $\hat{p} = \vec{p}/|\vec{p}|$ is the unit vector. Inserting the *ansatz* Eq.(2.4) into Eq.(2.3) leads to the explicit form

$$S(p_0, \vec{p}) = \frac{p_0 \gamma_0 - \vec{\gamma} \cdot \hat{p}(p + \Sigma^V(p)) + \Sigma^S(p)}{p_0^2 - [(p + \Sigma^V(p))^2 + (\Sigma^S(p))^2]} \quad (2.5)$$

for the propagator, which, when inserted into Eq.(2.2), leads to the coupled set of non-linear integral equations,

$$\Sigma^S(p) = \frac{2}{3} \int \frac{d^3 k}{(2\pi)^3} V(\vec{p} - \vec{k}) \frac{\Sigma^S(k)}{[(k + \Sigma^V(k))^2 + (\Sigma^S(k))^2]^{1/2}} \quad (2.6)$$

$$\Sigma^V(p) = \frac{2}{3} \int \frac{d^3 k}{(2\pi)^3} V(\vec{p} - \vec{k}) \frac{(k + \Sigma^V(k)) \hat{p} \cdot \hat{k}}{[(k + \Sigma^V(k))^2 + (\Sigma^S(k))^2]^{1/2}} \quad (2.7)$$

for the unknown scalar and vector self-energies. The form of Eq.(2.5) and also (2.7) suggests a reparametrization of $\Sigma^S(p)$ and $\Sigma^V(p)$ as

$$\Sigma^S(p) = E(p) \sin \phi(p) \quad (2.8a)$$

$$\text{and } p + \Sigma^V(p) = E(p) \cos \phi(p) \quad (2.8b)$$

introducing the variable $E(p)$ and the angular variable $\phi(p)$. It can be seen that the variable $E(p)$ plays the role of an energy, by writing the propagator with respect to the new variables:

$$S(p_0, \vec{p}) = \frac{\gamma^0 p_0 - \vec{\gamma} \cdot \hat{p} E(p) \cos(\phi(p)) + E(p) \sin(\phi(p))}{p_0^2 - E(p)^2}, \quad (2.9)$$

while the Eqs.(2.8) are replaced by

$$E(p) \sin(\phi(p)) = \frac{2}{3} \int \frac{d^3 k}{(2\pi)^3} V(\vec{p} - \vec{k}) \sin(\phi(k)) \quad (2.10a)$$

$$E(p) \cos(\phi(p)) - p = \frac{2}{3} \int \frac{d^3 k}{(2\pi)^3} V(\vec{p} - \vec{k}) \cos(\phi(k)) \hat{p} \cdot \hat{k}. \quad (2.10b)$$

A simple manipulation of Eqs.(2.10) can be made to decouple the unknowns $E(p)$ and $\phi(p)$, leading to the result

$$p \sin(\phi(p)) = \frac{2}{3} \int \frac{d^3 k}{(2\pi)^3} V(\vec{p} - \vec{k}) [\sin(\phi(k)) \cos(\phi(p)) - \hat{p} \cdot \hat{k} \cos(\phi(k)) \sin(\phi(p))], \quad (2.11)$$

that determines $\phi(p)$ solely. One may note that the chiral condensate can be expressed purely in terms of $\phi(p)$ as

$$\langle \bar{\psi}\psi \rangle = -\frac{3}{\pi^2} \int_0^\infty dk k^2 \sin(\phi(k)), \quad (2.12)$$

from which it is clear that $\phi(p)$ is the order parameter characterizing a non-trivial ground state. The determining equation for this function, Eq.(2.11) is thus the *gap equation* for an arbitrary potential in this model. Assuming that the symmetry breaking is maximal for the particle at rest, one may impose the boundary conditions

$$\lim_{p \rightarrow 0} \phi(p) = \frac{\pi}{2}, \quad (2.13)$$

while for large p ,

$$\lim_{p \rightarrow \infty} \phi(p) \rightarrow 0. \quad (2.14)$$

This completely specifies the problem.

B. Confinement, physical and unphysical variables

While the formal manipulations of the previous section are simple, some interpretation of the derived equations is required for a potential that is confining. In particular, the simple form of the propagator in Eq.(2.9) might lead one to believe that this function has singularities in the complex plane. In fact, this is not so. Closer inspection of the defining relation for $E(p)$ in Eq.(2.10) indicate that it is related to the integral of the function $V(\vec{p} - \vec{k})$, which, for a confining potential, is infrared singular. Thus $E(p)$ may *not* be interpreted as the physical energy of a quark. Only variables that are found to be infrared finite (and, if necessary, ultraviolet renormalizable) can be regarded in a physical sense [10].

We thus assert that: (i) $E(p)$ is, in general, divergent, and thus necessitates a redefinition of the physical energy in order to extract a physical quasiparticle mass, and (ii) $\phi(p)$ is a physical quantity for both linear and quadratic confining potentials, as the gap equation that it satisfies is infrared finite. In the following two subsections, we examine the possible divergences that may be associated with the infrared, $\vec{k} \rightarrow 0$ and ultraviolet $k \rightarrow \infty$ behavior of the gap and energy equations respectively.

1. Ultraviolet divergences

a. Gap Equation For $p \rightarrow \infty$, $\sin(\phi(p)) \rightarrow 0$ and $\cos(\phi(p)) \rightarrow 1$. The first term of the gap equation, Eq.(2.11) is thus ultraviolet convergent. A divergence could however arise from the second term, depending on the form of the potential. For a Coulomb-like potential of the form $V(r) \sim -1/r$ or $V(q) \sim 1/q^2$, a divergence going as

$$\int d^3k \frac{1}{k^2} \sim \int dk k^2 \frac{1}{k^2} \quad (2.15)$$

occurs. In general, the gap equation is ultraviolet divergent for potentials that fall off more weakly than the Coulomb potential. In order to quantify this statement, consider a potential of the general form $V = V(|\vec{p} - \vec{k}|^2)$. The leading k dependence is obtained from the Taylor series of this function about $\vec{p} = 0$, as

$$V(|\vec{p} - \vec{k}|^2) = V(k^2) - 2\vec{p} \cdot \vec{k} \frac{\partial V(k^2)}{\partial(k^2)} + \dots \quad (2.16)$$

and inserting this into the divergent term of the gap equation

$$\frac{2}{3} \int \frac{d^3k}{(2\pi)^3} V(|\vec{p} - \vec{k}|^2) \hat{p} \cdot \hat{k} \sin(\phi(p)), \quad (2.17)$$

one sees, after performing the angular integration that the leading possibly divergent contribution goes as

$$\int d^3k \frac{\partial V(k^2)}{\partial(k^2)} k. \quad (2.18)$$

For a confining potential that has the limiting behavior

$$V(q^2) \stackrel{q \rightarrow \infty}{\sim} (q^2)^{-\alpha}, \quad \alpha > 0, \quad (2.19)$$

Eq.(2.18) can be evaluated to give the result $k^{-2\alpha+2}/(-2\alpha+2)$, which thus exhibits a divergence for $\alpha \leq 1$. Denoting

$$Z - 1 = -\frac{4}{9} \int \frac{d^3k}{(2\pi)^3} \frac{\partial V(k^2)}{\partial(k^2)} k, \quad (2.20)$$

one finds that the divergent part of the gap equation, i.e. Eq.(2.17), is of the form

$$\text{divergence} = (Z - 1)p \sin(\phi(p)). \quad (2.21)$$

This, however, has exactly the form that appears on the left hand side of the gap equation, and thus any ultraviolet divergences can be simply compensated by introducing an appropriate counter term into the Hamiltonian, in this case,

$$\Delta\hat{H} = (Z - 1) \int d^3x \hat{\psi}^\dagger(\vec{x}) (-i\vec{\alpha} \cdot \nabla) \hat{\psi}(\vec{x}). \quad (2.22)$$

With this renormalization prescription, ultraviolet divergences can be unambiguously dealt with.

b. Energy equation Since $\phi(k) \rightarrow 0$ when $k \rightarrow \infty$, it follows from Eq.(2.10) that $E(p)$ is ultraviolet convergent.

2. Infrared divergences

a. Gap equation By performing an expansion of the bracketed term in the integrand of Eq.(2.11) about $p = k$, i.e.

$$\begin{aligned} \sin(\phi(k)) \cos(\phi(p)) - \hat{p} \cdot \hat{k} \cos(\phi(k)) \sin(\phi(p)) \\ = (\vec{p} - \vec{k}) \cdot \hat{p} \phi'(p) + O((\vec{p} - \vec{k})^2), \end{aligned} \quad (2.23)$$

and shifting the variable $\vec{q} = \vec{p} - \vec{k}$ in the integrand of the gap equation one may isolate the possible divergence as being

$$\text{divergence} \sim \frac{2}{3} \int \frac{d^3q}{(2\pi)^3} V(\vec{q}) O(q^2). \quad (2.24)$$

Thus, for a linear confining potential, $V(r) \sim r$ or $V(q) \sim 1/q^4$, this term takes the form

$$\int d^3q \frac{1}{q^4} O(q^2) \sim \int dq q^2 \frac{1}{q^4} O(q^2) \sim \int dq, \quad (2.25)$$

which is infrared finite. Thus the gap equation is non-singular in the infrared in this case. This can also be verified to be true for a potential that is quadratically confining, i.e. $V(r) \sim r^2$.

b. Energy equation Eq.(2.10) can be used to determine the quasiparticle energy,

$$E(p) = \frac{2}{3} \int \frac{d^3k}{(2\pi)^3} V(|\vec{p} - \vec{k}|) \frac{\sin(\phi(k))}{\sin(\phi(p))} = \frac{2}{3} \int \frac{d^3k}{(2\pi)^3} V(k) \frac{\sin(\phi(|\vec{p} - \vec{k}|))}{\sin(\phi(p))}. \quad (2.26)$$

The divergence structure in the infrared follows on expanding the sine function about $\vec{k} = \vec{p}$. The leading term is

$$\begin{aligned} \text{divergent part of } E(p) &\sim \frac{2}{3} \int \frac{d^3 k}{(2\pi)^3} V(k) \\ &\sim \text{divergent part of } E(0), \end{aligned} \quad (2.27)$$

the latter statement of which can be seen by inspection. It is thus evident that the energy *difference*

$$E(p) - E(0) \quad (2.28)$$

is infrared finite.

One may note that the subtraction of the infinite zero point energy corresponds to shifting the potential by an infinite constant

$$V(\vec{r}) \rightarrow V(\vec{r}) - \frac{2}{3} \int \frac{d^3 k}{(2\pi)^3} V(k) \quad (2.29)$$

or

$$V(\vec{q}) \rightarrow V(\vec{q}) - (2\pi)^3 \delta^{(3)}(\vec{q}) \frac{2}{3} \int \frac{d^3 k}{(2\pi)^3} V(k). \quad (2.30)$$

Thus the content of this section on infrared divergences can also be viewed in the context that physical observables are invariant under shifts of the potential by a constant. This is immediately obvious for the gap equation, Eq.(2.11), but not for $E(p)$ alone as in Eq.(2.26). Under the general shift

$$V(\vec{r}) \rightarrow V(\vec{r}) + U, \quad (2.31)$$

it follows that $E(p) \rightarrow E(p) + 2U/3$. Consequently, the determination of $E(0)$ does not provide a unique determination of the quasiparticle mass. Following Ref. [10], one may make an identification of the quasiparticle mass by rewriting the single particle Green function of Eq.(2.5) as

$$S(p_0, \vec{p}) = \frac{R_+(\vec{p})}{p_0 + (E(p) - E(0)) + E(0)} + \frac{R_-(\vec{p})}{p_0 - (E(p) - E(0)) - E(0)}, \quad (2.32)$$

where the residues

$$R_{\pm}(\vec{p}) = \frac{1}{2}(\gamma_0 \mp \vec{\gamma} \cdot \hat{p} \cos(\phi(p)) \pm \sin(\phi(p))) \quad (2.33)$$

are *unaffected* by a shift in the potential. By comparing the residues at low momenta with those of a free relativistic particle of mass m^* , viz. $R_{\pm}^0 = \frac{1}{2}(\gamma^0 \mp \vec{\gamma} \cdot \vec{p}/m^* \pm 1)$, one arrives at an unambiguous identification

$$\frac{1}{m^*} = \lim_{p \rightarrow 0} \frac{\cos(\phi(p))}{p} \quad (2.34)$$

for the quasiparticle mass.

It is however physically more intuitive to introduce the *shifted* energy

$$\bar{E}(p) = E(p) - E(0) + m^* \quad (2.35)$$

which has the desirable property $\bar{E}(0) = m^*$. In order to ensure this property, the shift

$$\frac{2}{3}U = -E(0) + m^* \quad (2.36)$$

must be invoked in the potential Eq.(2.31).

In concluding this section, we point out that both m^* and the condensate $\langle \bar{\psi}\psi \rangle$, calculated via Eqs.(2.34) and (2.12) respectively, fulfil the requirements of being physical observables as they are solely functions of the gap variable ϕ .

III. SOLUTIONS FOR QUADRATIC CONFINEMENT AT $T = 0$

In this section, we illustrate the solution of the gap equation for a quadratically confining potential, since such a form for the potential has the advantage that the integral gap and energy equations can be reduced to differential forms, even although they are highly non-linear, and the problem is a boundary value, not an initial value one. Nevertheless, many analytic techniques are at ones disposal, and in this case, precise solutions can be found. Note that this problem has been solved approximately elsewhere [16], but not within the physical framework presented here. Here we give a more general solution than that in Ref. [16]. Since the method will also be applied to the problem at finite temperatures in Section IV, we do this in some detail.

Our starting point is the attractive potential

$$V(\vec{r}) = -\lambda \vec{r}^2 + U, \quad (3.1)$$

with $\lambda > 0$ controlling the effective strength of the potential, and U determined via the condition Eq.(2.36). This potential is binding in the quark-antiquark channel. The Fourier transform of the potential Eq.(3.1) is given as

$$V(\vec{q}) = \lambda(2\pi)^3 \nabla_q^2 \delta^{(3)}(\vec{q}) + U(2\pi)^3 \delta^{(3)}(\vec{q}). \quad (3.2)$$

Inserting this into the integral gap equation, Eq.(2.11) and performing an integration by parts, leads one to the differential form

$$p \sin(\phi(p)) = \frac{2}{3} \lambda (\phi''(p) + \frac{2}{p} \phi'(p) + \frac{1}{p^2} \sin(2\phi(p))), \quad (3.3)$$

which is to be solved subject to the boundary conditions Eqs.(2.13) and (2.14). A semi-analytic solution to this problem is presented in the following subsection. This is later compared with an exact numerical solution.

Semi-analytic solution

The differential gap equation, written as

$$ap^3 \sin(\phi(p)) = p^2 \phi''(p) + 2p \phi'(p) + \sin(2\phi(p)) \quad (3.4)$$

with $a^{-1} = 4\lambda/3 > 0$ can be solved by the technique of asymptotic matching [24]. In this method, one identifies overlapping regions in the independent variable, for which exact analytic solutions can usually be obtained. On enforcing the boundary conditions, these solutions are matched onto one another asymptotically in their common region of validity. Four such regions can be identified, of which the second and fourth are a limiting cases of the third and are thus not independent. These regions are

$$(1) \ p \rightarrow 0 \quad \Rightarrow \quad p^2 \phi''(p) + 2p \phi'(p) = -\sin(2\phi(p)) \quad (3.5a)$$

$$(2) \ p \text{ and } \phi(p) \text{ small} \quad \Rightarrow \quad p^2 \phi''(p) + 2p \phi'(p) = -2\phi(p) \quad (3.5b)$$

$$(3) \ \phi(p) \text{ small for arbitrary } p \quad \Rightarrow \quad p^2 \phi''(p) + 2p \phi'(p) = (ap^3 - 2)\phi(p) \quad (3.5c)$$

$$(4) \ \phi(p) \text{ small and } p \rightarrow \infty \quad \Rightarrow \quad p^2 \phi''(p) + 2p \phi'(p) = ap^3 \phi(p). \quad (3.5d)$$

Correspondingly, the energy equation, in differential form, is given as

$$\bar{E}(p) = -\frac{1}{a}(\phi'(p))^2 + \frac{2}{p^2} \cos^2(\phi(p)) + p \cos(\phi(p)) + \frac{2}{3}U. \quad (3.6)$$

Thus, once one has knowledge of $\phi(p)$, the energy may be immediately determined.

We now deal with each of the above cases in turn.

case 1 : The determining equation Eq.(3.5a) in this case cannot be solved exactly due to non-linearities. However, since the boundary condition Eq.(2.13) must be imposed, it is useful to write $\phi(p) = \pi/2 + \epsilon(p)$ with $\epsilon(0) = 0$. One may insert this *ansatz* into Eq.(3.5a) and solve the resulting equation exactly for small ϵ . The non-divergent solution is found to be linear in p so that one may write, in leading order,

$$\phi(p) \simeq \frac{\pi}{2} + cp + \eta(p), \quad p \rightarrow 0, \quad \eta(0) = 0 \quad (3.7)$$

where c is as yet an undetermined constant. Clearly this procedure can be repeated by constructing the differential equation for $\eta(p)$ to obtain further corrections. This leads to the higher order correction $\eta(p) = bp^3 + O(p^4)$, with $b = (a - 4c^3/3)/10$. Note that the constant c in Eq.(3.7) plays an extremely important role. According to Eq.(2.34) and Eq.(3.7),

$$m^{*-1} = -\phi'(0) = -c, \quad (3.8)$$

i.e. the initial slope of the gap angle is related to the inverse quasiparticle mass, This determines c to be negative, $c = -|c|$.

We now turn to the determination of $\bar{E}(p)$. Using the approximation Eq.(3.7) in Eq.(3.6), one finds

$$\bar{E}(p) = -\frac{3c^2}{a} + [\frac{2c^4}{a} - 2c]p^2 + \frac{2}{3}U, \quad p \rightarrow 0. \quad (3.9)$$

The criterion that $\bar{E}(0) = m^*$ now fixes U to be

$$U = \frac{9}{2} \frac{c^2}{a} + \frac{3}{2} \frac{1}{|c|}. \quad (3.10)$$

It is interesting to note that, in light of these comments, the dispersion relation for $\bar{E}(p)$ for small momenta, from Eq.(3.8),

$$\bar{E}(p) = m^* + Bp^2, \quad p \rightarrow 0, \quad (3.11)$$

with $B = 2c^4/a - 2c > 0$, is non-relativistic.

case 2 : In the region specified as (2), the determining equation Eq.(3.5b) can be solved exactly. The solution is

$$\phi_2(p) = \frac{\gamma}{\sqrt{p}} \cos\left(\frac{\sqrt{7}}{2} \ln(p) + \delta\right) \quad (3.12)$$

where γ and δ are two constants of integration.

case 3 : The determining equation over this region, i.e. Eq.(3.5c) is a Bessel equation. Selecting the solution that falls off with momentum leads to the solution

$$\phi_3(p) = Bp^{-1/2}K_{i\sqrt{7}/3}(\frac{2}{3}\sqrt{a}p^{3/2}), \quad (3.13)$$

where $K_n(x)$ is the n th order modified Bessel function of the second kind, and B is an integration constant.

case 4 : Eq(3.5d) is a limiting case of Eq.(3.5c) and has as decaying solution, the modified Bessel function

$$\phi_4(p) = Cp^{-1/2}K_{1/3}(\frac{2}{3}\sqrt{a}p^{3/2}). \quad (3.14)$$

For large x , $K_n(x) \sim \sqrt{\frac{\pi}{2x}}e^{-x}[1 + O(1/x)]$, so that

$$\phi_4(p) \sim Ap^{-5/4}\exp(-\frac{2}{3}\sqrt{a}p^{3/2}) \quad (3.15)$$

in the limit $p \rightarrow \infty$.

We now turn to the energy determination. From Eq.(3.6), it follows that

$$\bar{E}(p) \stackrel{p \rightarrow \infty}{\sim} p. \quad (3.16)$$

Thus one recovers a relativistic dispersion relation at high momenta.

The next issue is to match all solutions that have been obtained piecewise to construct one continuous solution over the entire momentum range.

Asymptotic matching over the intervals. One may observe that the Eqs.(3.5a) and (b) are scale invariant, i.e. invariant under the transformation $p \rightarrow |c|p$. This enables one to determine the constants γ and δ for the solution (3.12) without actually knowing $c = \phi'(0)$. One determines the solution to Eq.(3.5a) with initial values

$$\phi_1(0) = \frac{\pi}{2} \quad \text{and} \quad \phi_1'(0) = -1, \quad (3.17)$$

and one considers this solution for $p \rightarrow \infty$. This is matched onto the solution $\phi_2(p)$ from Eq.(3.12) and the associated $\phi_2'(p)$ in the regime $p \rightarrow \infty$ of the $\phi_1(p)$ equation. This is possible since the solution of $\phi_2(p)$ can be matched to that of $\phi_1(p)$ down to small momenta. On the other hand, both Eqs.(3.5a) and (3.5b) have the same behavior in the limit $p \rightarrow 0$. One is thus able to extract the constants for the solution in region (2).

Numerically, one finds

$$\begin{aligned}\gamma &= 0.700460a^{-1/6} \\ \delta &= 0.238503.\end{aligned}\tag{3.18}$$

Now the solution in region (2), $\phi_2(p)$, must be matched onto the solution in region (3), $\phi_3(p)$. To do this, one requires $\phi_3(p)$, for $p \rightarrow 0$. Since

$$K_{i\nu} \stackrel{x \rightarrow 0}{\sim} \frac{1}{2}\Gamma(i\nu)\left(\frac{1}{2}x\right)^{-i\nu} + c.c.,\tag{3.19}$$

one finds

$$\phi_3(p) \stackrel{p \rightarrow 0}{\sim} Bp^{-1/2}|\Gamma(\frac{\sqrt{7}}{3})|\frac{1}{2}[\exp(i\frac{\sqrt{7}}{3}\ln(\frac{\sqrt{a}}{3}p^{3/2}) - i\rho) + c.c.] \tag{3.20}$$

$$= Bp^{-1/2}|\Gamma(\frac{\sqrt{7}}{3})|\cos(\frac{\sqrt{7}}{2}\ln(p) + \frac{\sqrt{7}}{2}\ln(\frac{a^{1/3}}{3}) - \rho), \tag{3.21}$$

where $\rho = \arg(\Gamma(\frac{i\sqrt{7}}{3})) \simeq -1.877978$. The full, non-scaled solution in region (2),

$$\phi_2(p) = \frac{\gamma}{\sqrt{|c|p}}\cos(\frac{\sqrt{7}}{2}\ln(|c|p) + \delta) \tag{3.22}$$

can be directly compared with Eq.(3.21), to give

$$\delta + \frac{\sqrt{7}}{2}\ln|c| = \frac{\sqrt{7}}{2}\ln(\frac{a^{1/3}}{3}) - \rho + n\pi \tag{3.23}$$

and

$$\frac{\gamma}{\sqrt{|c|}} = B|\Gamma(i\frac{\sqrt{7}}{3})|. \tag{3.24}$$

One may now extract the slope $|c|$ from Eq.(3.23). Explicitly, one has

$$|c| = \frac{a^{1/3}}{3}\exp\frac{2}{\sqrt{7}}(n\pi - \rho - \delta). \tag{3.25}$$

where n is the number of nodes occurring in the solution. In Table I, we list the node and the value for c that were extracted via this asymptotic matching procedure via expression (3.25) in comparison with a trial exact procedure in which one attempts to solve the full equation starting as near to the origin as is numerically permissible.

In Fig.2, we show the nodeless solution for the gap parameter. The analytic solution in regions (1), (2) and (3) are indicated on the graph by various symbols. One

notes that the approximation is in excellent agreement with the numerical result. This procedure has proven extremely useful both as a check but also in guiding the numerical solutions, since the gap equation is highly non-linear. Figure 3 indicates the first three solutions for $\phi(p)$. One notes that the slope at the origin increases sharply with the number of nodes, indicating that a succession of values of m^* exist that *decrease* with the number of nodes.

Energy Density. In order to determine which of the solutions, i.e. that with no node present or alternatively with multiple nodes present should give rise to the ground state of the system, one needs to evaluate the change in the energy density that occurs in going from the normal vacuum to the condensed one. The physical solution to the gap equation is then determined as the solution that lowers the energy the most. The vacuum energy density in the condensed phase, $W_{condensed} = \langle cond|H|cond \rangle$ or in the normal phase, $W_{normal} = \langle 0|H|0 \rangle$, can be obtained directly from the appropriate single particle Green's function, via the formula [25]

$$W_{c,n} = -\frac{i}{2} \int \frac{d^4p}{(2\pi)^4} Tr[\gamma^0 p_0 + \vec{\gamma} \cdot \vec{p}] S_{c,n}(p_0, \vec{p}) e^{i\eta p_0} \quad (3.26)$$

where c, n refer to the condensed or normal phases respectively. This equation is general and exact for a four-point or two-body interaction, such as that under study here. Explicitly inserting the Green function, Eq.(2.32), for the condensed phase and the free Green function for the normal phase, one finds the expression

$$\Delta W = W_c - W_n = \frac{3}{2\pi^2} \int_0^\infty dp p^2 [2p(1 - \cos(\phi(p))) - \frac{1}{ap^2} \sin^2 \phi(p) + \frac{1}{2a} \phi'^2(p)] \quad (3.27)$$

for the change in energy density in moving from the normal to condensed vacua. A numerical analysis indicates that ΔW is negative, and that the nodeless solution, i.e. the solution with the smallest slope or largest mass, always leads to the lowest energy state.

IV. FINITE TEMPERATURE

To date, there have been several studies of the finite temperature gap equation. These differ markedly in (a) the gap equation actually proposed or derived and the subsequent interpretation of the variables, and (b) the form of the potential chosen

for studying this model. In the first part (a), there can of course be only one correct equation. In analogy to the $T = 0$ case, it can be formally derived by one of two equivalent methods, the Green function approach, similar to that followed at $T = 0$ in Section II of this paper, or via a variational method that proceeds by constructing the Gibbs free energy and minimizing it with respect to a variational parameter, see Ref. [17]. In this section, we will take the former approach, since the generalization from Section II is evidently simple. We contrast this result with the conflicting postulated gap equations of other authors [13] and interpret the quasiparticle energy that occurs along the lines of Refs. [10] and [12].

With regard to point (b) above, let us mention that the only attempt to date of extracting a numerical solution to a finite temperature gap equation (not that derived here) employs an *a priori* temperature dependent coupling strength for a Coulomb-like potential [13]. This, in itself, presents difficulties in the construction of a consistent thermodynamic description. In the case handled, the second order phase transition that was observed was due to the coupling, that strongly modifies the infrared behavior of the potential, rather than the inherent temperature dependence of the quasiparticle energy, which was omitted in this description.

An additional difficulty manifests itself in the finite temperature formalism with regard to the zero temperature one. Since statistical averages over a grand canonical ensemble are made, all states are included in the averaging process. However, physical states should be colorless. Imposing this restriction leads to rather complex technicalities and a complex set of equations, from which it is not evident what the physics actually is [17]. Taking the point of view that the restriction to color singlet space should cause changes of at most 10–20%, but should not induce radical differences otherwise [26], we attempt to solve the gap equations that are derived without this restriction and which have a physical constraint imposed upon the quasiparticle energy. We do this using the confining potential that was introduced in Section III, following the analysis of this section rather closely.

We proceed by briefly deriving the finite temperature gap equation.

A. Gap equation

The Green function approach that was detailed in Section II can be simply generalized to finite temperatures in order to derive the associated gap equation. Here, using the Matsubara or imaginary time propagator,

$$S_\beta(i\omega_n, \vec{p}) = \frac{1}{i\omega_n \gamma_0 - \vec{\gamma} \cdot \vec{k} - \Sigma_\beta(\vec{k})}, \quad (4.1)$$

where $\omega_n = (2n + 1)\pi/\beta$, $n = 0, \pm 1, \pm 2, \pm 3, \dots$, and the self-energy $\Sigma_\beta(\vec{k})$ is again decomposable into a vector and scalar piece, $\Sigma_\beta(\vec{k}) = \Sigma_\beta^S(\vec{k}) + \vec{\gamma} \cdot \hat{k} \Sigma_\beta^V(\vec{k})$, one may write

$$\Sigma_\beta(p) = -\frac{1}{\beta} \sum_{a=1}^8 \sum_n \int \frac{d^3k}{(2\pi)^3} V(\vec{p} - \vec{k}) \gamma^0 \frac{\lambda^a}{2} S_\beta(i\omega_n, \vec{k}) \gamma_0 \frac{\lambda^a}{2}, \quad (4.2)$$

on interpreting the Fock diagram of Fig.2. Now the steps that were performed in Section II leading to Eq.(2.10) can be similarly executed here, once the Matsubara sum has been performed. Eqs.(2.10a) and (2.10b) are replaced by their temperature generalizations,

$$E_\beta(p) \sin(\phi_\beta(p)) = \frac{2}{3} \int \frac{d^3k}{(2\pi)^3} V(\vec{p} - \vec{k}) \sin(\phi_\beta(k)) \tanh\left(\frac{\beta}{2} E_\beta(k)\right) \quad (4.3a)$$

$$E_\beta(p) \cos(\phi_\beta(p)) - p = \frac{2}{3} \int \frac{d^3k}{(2\pi)^3} V(\vec{p} - \vec{k}) \hat{p} \cdot \hat{k} \cos(\phi_\beta(k)) \tanh\left(\frac{\beta}{2} E_\beta(k)\right). \quad (4.3b)$$

Note that a central issue in this derivation is that the self-energies $\Sigma_\beta^S(p)$ and $\Sigma_\beta^V(p)$ making up $\Sigma_\beta(p)$ are now necessarily a function of temperature. This temperature dependence is now relayed to the reparametrization functions $\phi_\beta(p)$ and $E_\beta(p)$ that are defined as in Eqs.(2.8), but which contain the explicit temperature labels. It has been noted that the simple procedure used previously to decouple these equations no longer functions [17,12]. The finite temperature gap equation, constructed by multiplying Eq.(4.3a) by $\cos(\phi_\beta(p))$, Eq.(4.3b) by $\sin(\phi_\beta(p))$ and subtracting, is

$$p \sin(\phi_\beta(p)) = \frac{2}{3} \int \frac{d^3k}{(2\pi)^3} V(\vec{p} - \vec{k}) [\sin(\phi_\beta(k)) \cos(\phi_\beta(p)) - \hat{p} \cdot \hat{k} \cos(\phi_\beta(k)) \sin(\phi_\beta(p))] \times \tanh\left(\frac{\beta}{2} E_\beta(k)\right). \quad (4.4)$$

This gap equation coincides with that of Refs. [12] and [17]. It differs however from that of Ref. [11] in that these authors regard $E_\beta = E$ as a constant, *independent* of

the temperature. In contrast, in Ref. [13], the authors use a gap equation similar to Eq.(4.4), but with the tanh factor entirely absent. These authors claim that the hyperbolic tangent function and energy dependence is irrelevant, arguing that $E(k)$ is infinite anyway. This argument is, however, too naive, and is not confirmed by our study, in which we first make use of *physical* arguments to shift the energy along the lines that were discussed in Section II: Note that, taken at face value, Eq.(4.4) taken together with Eq.(4.3a), violates the criterion that physical observables, such as $\phi_\beta(k)$ are invariant under a shift in the potential by a constant, as was easily seen to be the case in Section II at $T = 0$. This issue has been dealt with in detail in Refs. [12] and [17]. Both of these sets of authors show that this conflict can be resolved by suppressing color fluctuations and restricting the grand canonical ensemble trace to cover color singlet states only. The color projected gap equation [17] is however extremely difficult to solve, in particular, because of the temperature dependence of the energy. Note that the temperature dependence of the energy variable is crucial in the BCS theory of superconductivity for obtaining the correct temperature behavior of the gap parameter for a superconductor [27]. It is thus the purpose of this study to investigate the role of the temperature dependence of the energy function and its consequences.

Guided by the situation at $T = 0$, one may make a simple physical *ansatz*, that of replacing $E_\beta(p)$ in the tanh function of Eq.(4.4) by

$$\bar{E}_\beta(p) = E_\beta(p) - E_\beta(0) + m_\beta^*. \quad (4.5)$$

This is motivated, as in Section II following Ref. [10], by comparing the Green function in this case with the low momentum version of the free temperature Green function [12]. The real time forms are

$$\begin{aligned} S(\vec{p}, \omega) = & \left[\frac{R_{+,\beta}(p)}{\omega - E_\beta(p) + i\eta} + \frac{R_{-,\beta}(p)}{\omega + E_\beta(p) - i\eta} \right] \\ & + 2\pi i f[\beta E_\beta(p)] [\gamma^0 \omega - \vec{\gamma} \cdot \hat{p} E_\beta(p) \cos(\phi_\beta(p)) + E_\beta(p) \sin(\phi_\beta(p))] \delta(\omega^2 - E_\beta^2(p)), \end{aligned} \quad (4.6)$$

for the full Green function, with

$$R_{\pm,\beta}(p) = \frac{1}{2} [\gamma^0 \mp \vec{\gamma} \cdot \hat{p} \cos(\phi_\beta(p)) \pm \sin(\phi_\beta(p))], \quad (4.7)$$

where $f(x) = 1/(\exp(\beta x) + 1)$ and $\eta \rightarrow 0^+$, while the free Green function has the form

$$S_{free} = \frac{R_{+,\beta}^0(p)}{\omega - m_\beta^* + i\eta} + \frac{R_{-,\beta}^0(p)}{\omega + m_\beta^* - i\eta} + 2\pi i f(\beta m_\beta^*) [\gamma_0 \omega - \vec{\gamma} \cdot \vec{p} + m_\beta^*] \delta(\omega^2 - m_\beta^2) \quad (4.8)$$

with $R_{\pm,\beta}^0(p) = \frac{1}{2}(\gamma^0 \mp \vec{\gamma} \cdot \vec{p}/m_\beta^* \pm 1)$.

Thus one recovers the identifying criterion

$$\lim_{p \rightarrow 0} \frac{\cos(\phi_\beta(p))}{p} = \frac{1}{m_\beta^*} \quad (4.9)$$

that generalizes Eq.(2.34) to finite temperatures, as well as the essential condition

$$E_\beta(p) \rightarrow \bar{E}_\beta(p) \rightarrow m_\beta^*, \quad p \rightarrow 0 \quad (4.10)$$

that has prompted the replacement Eq.(4.5). Given Eq.(4.5), one recovers the expected physical quasiparticle properties.

The associated finite temperature condensate density is determined to be

$$\langle \bar{\psi} \psi \rangle_\beta = -\frac{3}{\pi^2} \int_0^\infty dk k^2 \sin(\phi_\beta(k)) \tanh\left(\frac{\beta}{2} \bar{E}_\beta(k)\right), \quad (4.11)$$

which will be evaluated in the following section for the potential for quadratic confinement.

B. Quadratic Confinement

The purpose of this section is to examine the temperature dependence of the gap function and the self-energies for the quadratically confining potential of Eq.(3.1) and its Fourier transform, Eq.(3.2). In this section, the strategy is to implement Eq.(4.5) in an approximate fashion that highlights the temperature dependence of the quasiparticle energy. We proceed once again by bringing the gap equation into differential form. One finds that Eq.(3.4) has the generalized form

$$ap^3 \sin(\phi_\beta(p)) \coth\left(\frac{\beta}{2} \bar{E}_\beta(p)\right) = p^2 \phi''_\beta(p) + 2p \phi'_\beta(p) + \sin(2\phi_\beta(p)) + 2p^2 \frac{\beta \bar{E}_\beta'(p)}{\sinh(\beta \bar{E}_\beta(p))} \phi_\beta'(p), \quad (4.12)$$

while the energy equation, Eq.(3.6) is generalized to read

$$\begin{aligned}\bar{E}_\beta(p) = & -\frac{1}{a}(\phi_\beta'(p)^2 + \frac{2}{p^2} \cos^2(\phi_\beta(p))) \tanh(\frac{\beta}{2}\bar{E}_\beta(p)) + p \cos(\phi_\beta(p)) \\ & + \frac{1}{ap}[p \tanh(\frac{\beta}{2}\bar{E}_\beta(p))]'' + \frac{2}{3}U \tanh(\frac{\beta}{2}\bar{E}_\beta(p)).\end{aligned}\quad (4.13)$$

Unlike the system of equations (3.4) and (3.6) at zero temperature, one sees that Eqs.(4.12) and (4.13) are coupled non-linear differential equations in the two variables ϕ_β and \bar{E}_β . While it is possible to make a simple analysis for high temperatures and low/high momenta, it is a difficult problem to solve these two equations exactly. We thus do not attempt to do so here. After discussing the limits just mentioned, we shall investigate the role of an *assumed* temperature dependent dispersion relation for the energy, that allows us to decouple these equations and solve them.

c. High temperature limit. If, as $T \rightarrow \infty$, $\bar{E}_\beta(p)$ remains finite, then from Eq.(4.12),

$$p \sin(\phi_{\beta \rightarrow 0}(p)) = 0 \quad \text{for all } p \quad (4.14)$$

so that

$$\phi_{\beta \rightarrow 0}(p) = 0. \quad (4.15)$$

Consequently, from Eq.(4.13), it follows that $\bar{E}_{\beta \rightarrow 0} = p$ for all p , and one recovers the chiral limit.

d. Small momenta. Using the boundary conditions, $\bar{E}_\beta(0) = m_\beta$ and $\phi_\beta(0) = \pi/2$, one can expand $\phi_\beta(p)$ and $\bar{E}_\beta(p)$ in the small momentum region,

$$\phi_\beta(p) = \frac{\pi}{2} + c_1^\beta p + c_2^\beta p^2 + \dots \quad (4.16a)$$

$$\bar{E}_\beta(p) = m_\beta + a_1^\beta p + a_2^\beta p^2 + \dots \quad (4.16b)$$

where, from Eq.(4.9),

$$c_1^\beta = -\frac{1}{m_\beta^*} = c_\beta. \quad (4.17)$$

One may insert these expansions into Eq.(4.13). A necessary condition that $\bar{E}_\beta(p)$ does not diverge as $p \rightarrow 0$ is that $a_1^\beta = 0$. Thus one regains the observed $T \rightarrow 0$ dependence of Section III that

$$\bar{E}_\beta(p) = m_\beta^* + a_2^\beta p^2, \quad \text{for } p \rightarrow 0, \quad (4.18)$$

this equation being the analog of Eq.(3.11). As in that case, one may continue the expansion for $\phi_\beta(p)$, writing

$$\phi_\beta(p) = \frac{\pi}{2} + c^\beta p + \eta_\beta(p), \quad \text{with } \eta_\beta(0) = 0. \quad (4.19)$$

Inserting this and Eq.(4.16b) into the gap equation enables one to find a differential equation for $\eta_\beta(p)$ which has the solution $\eta_\beta(p) = b^\beta p^3$, with

$$b^\beta = \frac{1}{10} \left[a \coth(\beta/2|c^\beta|) + \frac{4\beta a_2^\beta |c^\beta|}{\sinh(\beta/2|c^\beta|)} + \frac{4}{3} (|c^\beta|)^3 \right]. \quad (4.20)$$

The coefficient a_2^β of the energy expansion may also be determined by inserting the expansions for \bar{E} and ϕ into Eq.(4.13). One finds

$$a_2^\beta = \frac{1}{3} [3|c^\beta|^2 \tanh(\beta/2|c^\beta|) + a(\frac{1}{|c^\beta|} - \frac{2}{3} U \tanh(\beta/2|c^\beta|))] \frac{1}{\beta} \cosh^2(\beta/2|c^\beta|). \quad (4.21)$$

Thus the behavior of ϕ_β and \bar{E}_β for small momenta is similar to that obtained at $T = 0$, see Section III.

e. Large momenta. From Eq.(4.13), it follows that, at large momenta, $\bar{E}_\beta(p) \sim p$, $p \rightarrow \infty$, and one no longer has a temperature dependence in this quantity. Thus the gap equation is precisely that of the zero temperature case.

As has been seen at zero temperature, and now also at finite values of the temperature, the dispersion relation for the energy is non-relativistic in the low momentum regime, but relativistic for high momenta. This is commensurate with a general relativistic *ansatz* for the quasiparticle energy. In the following, we will discuss the solution to the gap equation for two possible *ansätze*: (i) momentum independent, but temperature dependent,

$$\bar{E}_\beta(p) = m_\beta^* \quad (4.22)$$

and (ii) the relativistic dispersion relation,

$$\bar{E}_\beta(p) = \sqrt{m_\beta^{*2} + p^2}. \quad (4.23)$$

Note that *ansatz* (i), being totally devoid of momentum dependence, serves to highlight the influence of the *temperature* dependence of the energy variable on determining the features of the solution to the gap equation. In addition, the simplicity

of this *ansatz* allows us to solve the resulting equations easily. The second *ansatz*, while meeting physical expectations more readily, leads to equations that are somewhat more difficult to solve. As shall become evident, the results obtained from the second *ansatz* do not differ qualitatively from that of *ansatz* (i). This appears to indicate that the momentum dependence is secondary in comparison to a correct treatment of the implicit temperature behavior of the quasiparticle energy. Our two choices are detailed in the following two subsections.

C. Momentum independent ansatz

In this subsection, we examine the solution of the temperature dependent gap equation under the *ansatz* Eq.(4.22). This is interesting to study since it contains the essential ingredient, i.e. temperature dependence, that has previously been overlooked. Furthermore, the resulting transcendental equation is simple to solve. Let us be more precise. Inserting Eq.(4.22) into Eq.(4.12) leads to the result

$$a^\beta p^3 \sin(\phi_\beta(p)) = p^2 \phi_\beta''(p) + 2p\phi_\beta(p) + \sin(2\phi_\beta(p)), \quad (4.24)$$

with

$$a^\beta = a \coth\left(\frac{\beta}{2}m_\beta^*\right). \quad (4.25)$$

Except for the cotangent factor, this equation is identical with the $T = 0$ equation, Eq.(3.4). It may thus be treated semi-analytically in the same fashion. In particular, the relation Eq.(3.25) is valid, with c replaced by c^β and a replaced by a^β , i.e.

$$|c^\beta| = \frac{(a^\beta)^{1/3}}{3} \exp\left(\frac{2}{\sqrt{7}}(n\pi - \rho - \delta)\right). \quad (4.26)$$

Now, inserting a^β from Eq.(4.25) into this equation leads to the simple result

$$|c^\beta| = \left(\coth\left(\frac{\beta}{2}m_\beta^*\right)\right)^{1/3} |c|, \quad (4.27)$$

which, together with identification $|c^\beta| = 1/m_\beta^*$ and $|c| = 1/m^*$, leads to the transcendental equation

$$m_\beta^* = m^* (\tanh(\frac{\beta}{2}m_\beta^*))^{1/3} \quad (4.28)$$

that determines m_β^* . In addition to the trivial solution, $m_\beta^* = 0$, this equation has a non-trivial solution that can be determined numerically. Following this, $\phi_\beta(p)$ is determined, and the condensate $\langle\bar{\psi}\psi\rangle$, from Eq.(4.11), can be shown to have the form

$$\langle\bar{\psi}\psi\rangle_\beta = \langle\bar{\psi}\psi\rangle_{T=0}(\tanh(\frac{\beta}{2}m_\beta^*))^2 \quad (4.29)$$

in relation to its zero temperature value.

In Fig.4, we show the values of $\phi_\beta(p)$ as a function of p for different values of the temperature, scaled with respect to the dynamically generated constituent quark mass. One notes from this figure that the slope increases with increasing temperature, indicating the fall off of the constituent quark mass. The temperature dependence of the condensate is shown in Fig. 5 as a function of the dimensionless variable T/m^* . One sees that it falls off strongly to zero as $T \rightarrow 0$: at $T/m^* = 2.0$, the value of the condensate is less than 5% of its value at the origin. However, the transition of the condensate is smooth and there is no evident critical temperature at which a phase transition that restores chiral symmetry occurs. This behavior is also evident in that of the quasiparticle mass, which is shown in Fig.5 as a function of T/m^* . This function decreases rapidly over the first unit of T/m^* , but thereafter drifts gradually to zero.

D. Relativistic dispersion relation

In this subsection, we investigate the use of a relativistic energy-momentum *ansatz*, viz. that of Eq.(4.23). For small values of p , this has the expansion

$$\bar{E}_\beta(p) \stackrel{p \rightarrow 0}{\approx} m_\beta^* + \frac{p^2}{2m_\beta^*} + O(p^4), \quad (4.30)$$

enabling one to identify the expansion coefficient of the energy as

$$a_2^\beta = \frac{1}{2m_\beta^*} = \frac{1}{2}|c^\beta|, \quad (4.31)$$

and that of the gap parameter, from Eq.(4.20). One then has

$$b^\beta = \frac{1}{10}[a \coth(\frac{\beta}{2|c^\beta|}) + \frac{2\beta|c^\beta|^2}{\sinh(\beta/|c^\beta|)} + \frac{4}{3}|c^\beta|^3]. \quad (4.32)$$

The estimate for the gap parameter, $\phi_\beta(p)$, for p small, thus enables one to perform a numerical integration starting at a value of p close to the origin. Fig. 6 shows the solution to the gap equation as a function of momentum at different values of the temperature. This bears close resemblance to the solution obtained in the previous case. The condensate, calculated numerically from Eq.(4.11), is shown in Fig. 7. As in the previous case, it goes to zero, but somewhat faster than in the previous case. Once again, no transition to a chirally symmetric phase is observed at a finite value of the temperature, although the fall off, for low temperatures, is steep.

E. Comparative analysis

It is useful to examine the results for the previous two calculations on one graph. In Fig. 8, we show the condensate as a function of the temperature, for two arbitrary choices of the mass at zero temperature, either $m^* = 200\text{MeV}$, or $m^* = 300\text{MeV}$. It is interesting to note that both assumptions for the dispersion relation lead to the same qualitative picture. Both curves fall rapidly initially. Instead of a phase transition occurring however, the curves flatten off and fall more gently to zero. One may speculate that a better form or exact solution of the coupled equations may in fact yield a chiral phase transition at a finite value of the temperature. In any event, it is heuristically evident that the temperature fluctuations alone could drive a phase transition. In view of the difficulties presented here, we must conclude that it is necessary to study temperature behavior of even simpler confining models.

The temperature behavior of the masses themselves is shown in Fig. 9. These are also decreasing with temperature, as occurs, for example, in the Nambu–Jona-Lasinio model, but no direct linear proportionality with the condensate is in evidence. The fact, however, that the quasiparticle masses are a function of temperature is an indication that this feature, which gives rise to dropping or rising composite particle masses, will continue to be an existing feature of a model that incorporates confinement and chiral symmetry and which one can hopefully solve exactly. It is to be believed that the solutions obtained here, which in both cases indicate a drop in the condensate energy, but no phase transition at finite temperature, are a consequence of the approximations that have been made.

V. SUMMARY AND CONCLUSIONS

In this paper, we have analysed the Coulomb gauge model with respect to the inclusion of a divergent potential. In this model, confinement is incorporated into the scalar sector of the vector four-potential, although there is no compelling reason why this should be done. The consequences for the quark propagator are discussed and an analysis of the divergences in the infrared sector as well as the ultraviolet is presented. The arguments of Adler and Davis [10] that physical quantities should be infrared finite, coinciding with the condition that a shift in the potential by a constant should not affect physical quantities for color singlet states is used as the determining criterion for physical observables. An interpretation of the quasiparticle mass is made, since the quasiparticle energy is necessarily divergent.

The finite temperature generalization of this model yields a gap equation which differs from that of several authors. The identification of the quasiparticle mass in the fashion that was done at $T = 0$ leads to a natural physical prescription that suggests the introduction of a non-divergent temperature dependent quasiparticle energy $\bar{E}_\beta(p) = E(p) - E(0) + m_\beta^*$, so that $\bar{E}_\beta(p) \rightarrow m_\beta^*$ as $p \rightarrow 0$. Even so, the complex set of coupled equations that one obtains for the gap parameter and the energy cannot be solved exactly. Since the issue of other authors has been to neglect the temperature dependence of the energy function and obtain alternatively that a phase transition can [13] or cannot [17] occur, we propose to investigate two simple dispersion forms for the quasiparticle energy that have an inherent temperature dependence. We find that, while there is no transition to a chirally symmetric phase at a finite value of the temperature, there is nonetheless a sharp drop in the condensate density or order parameter at some point. Whether this is endemic to a confining potential, or whether it is simply a consequence of the shortcomings of the approximations made, is as yet unknown and could be studied using other confining potentials, and simplifying models. It is perhaps therefore of interest to develop models that are closer in structure to that of Nambu and Jona-Lasinio, in order to understand these properties.

ACKNOWLEDGMENTS

We wish to thank P. Rehberg and J. Hübner for their criticisms and careful reading of the manuscript. This work has been supported in part by the Deutsche Forschungsgemeinschaft DFG under the contract number Hu 233/4-4, and by the German Ministry for Education and Research (BMBF) under contract number 06 HD 742.

REFERENCES

- [1] F. KARSCH, “Quark Gluon Plasma”, Edited by *R.C. Hwa*, (World Scientific, Singapore, 1990)
- [2] Y. NAMBU AND G. JONA-LASINIO, *Phys. Rev.* **122** (1961) 345
- [3] *For reviews, see* U. VOGL AND W. WEISE, *Prog. Part. Nucl. Phys.* **27** (1991) 195; S.P. KLEVANSKY, *Rev. Mod. Phys.* **64** (1992) 649; T. HATSUDA AND T. KUNIHIRO, *Phys. Rep.* **247** (1994) 241.
- [4] P. ZHUANG, J. HÜFNER AND S.P. KLEVANSKY, *Nucl. Phys.* **A576** (1994) 525.
- [5] *This problem was first addressed in detail by* V.N. GRIBOV, “Orsay lectures on confinement I and II”, hep-ph 9404332 and 9403218.
- [6] R.L. JAFFE AND K. JOHNSON, *Comments Nucl. Part. Phys.* **7** (1977) 107.
- [7] G.V. EFIMOV AND S. NEDELKO, *Phys. Rev.* **D51** (1995) 176.
- [8] M. BUBALLA AND S. KREWALD, *Phys. Lett.* **B294** (1992) 19.
- [9] J.R. FINGER AND J.E. MANDULA, *Nucl. Phys.* **B199** (1982) 168.
- [10] S.L. ADLER AND A.C. DAVIS, *Nucl. Phys.* **B244** (1984) 469.
- [11] A.C. DAVIS AND A.C. MATHESON, *Nucl. Phys.* **B246** (1984) 203.
- [12] S.P. KLEVANSKY AND R.H. LEMMER, *Phys. Rev.* **D38** (1988) 3559.
- [13] R. ALKHOFFER AND P.A. AMUNDSEN, *Phys. Lett.* **B187** (1987) 395.
- [14] R. ALKHOFFER AND P.A. AMUNDSEN, *Nucl. Phys.* **B306** (1988) 305.
- [15] R. ALKHOFFER, P.A. AMUNDSEN AND K. LANGFELD, *Z. Phys.* **C42** (1989) 199.
- [16] A. LE YAOUANC, L. OLIVER, O. PÈNE, AND J.-C. RAYNAL, *Phys. Rev.* **D29** (1984) 1233.
- [17] A. LE YAOUANC, L. OLIVER, O. PÈNE AND J.-C. RAYNAL, *Phys. Rev.* **D39** (1989) 924.

- [18] H.J. MUNCZEK AND A.M. NEMIROVSKY, *Phys. Rev.* **D28** (1983) 181.
- [19] C.D. ROBERTS AND A. G. WILLIAMS, *Prog. Part. Nucl. Phys.* **33** (1994) 447; M.R. FRANK AND C.D. ROBERTS, *Phys. Rev.* **D51** (1995) 390.
- [20] *see, for example*, E. LAERMANN, *in Proceedings of the Quark Matter 96 conference*, Heidelberg, Germany, *Nucl. Phys.*, to be published.
- [21] F. GROSS AND J. MILANA, *Phys. Rev.* **D43** (1991) 2401; *ibid.* **D45** (1992) 969.
- [22] P. MARIS, *Phys. Rev.* **D52**(1995) 6087.
- [23] K. LANGFELD AND M. RHO, *Nucl. Phys.* **A596** (1996) 451.
- [24] C.M. BENDER AND S.O. ORSZAG, *Advanced Mathematical Methods for Scientists and Engineers*, McGraw-Hill Book Company, 1978.
- [25] *This is the relativistic generalization of the similar expression for non-relativistic systems that can be found, for example, in* A.L. FETTER AND J.D. WALECKA, “Quantum Theory of Many Particle Systems”, (McGraw-Hill, San Francisco, 1971).
- [26] B. MÜLLER, “The physics of the quark-gluon plasma”, *in* “Lecture Notes in Physics”, Vol. 225, Springer-Verlag.
- [27] *See, for example, the reference given in* [25].

TABLE I

n	$ c_{asmt} $	$ c_{num} $
0	2.09169	2.03750
1	22.4837	22.4246
2	241.680	241.634
3	2597.84	2597.83
4	27924.4	27925.0
5	300161	300170

Table 1: Solutions for the slope c obtained via asymptotic matching of the approximate solutions, and via a numerical procedure. The symbol n denotes the number of nodes that the solution has.

FIGURE CAPTIONS

Fig. 1. Fock Feynman diagram for the self-energy.

Fig. 2. The nodeless solution for the gap angular variable is shown as a function of the scaled momentum $k = a^{1/3}p$. The semi-analytic solutions in regions (1), (2) and (3) are indicated by crosses, stars and circles respectively.

Fig. 3. The first three solutions for $\phi(k)$ with zero, one and two nodes, are shown as a function of the scaled momentum $k = a^{1/3}p$.

Fig. 4. The quasiparticle spectrum $\bar{E}_\beta(k)$ and the scalar and vector self-energies $\Sigma^S(k)$ and $\Sigma^V(k) + k$ are shown as a function of the scaled momentum $k = a^{1/3}p$.

Fig. 5. Solutions $\phi_\beta(p)$ as a function of p , in the approximation $\bar{E}_\beta = m_\beta^*$ for various values of the scaled temperature T/m^* . The upper curve corresponds to $T/m^* = 0$. Successive curves have the values $T/m^* = 0.2, 0.5, 1.0, 5.0$ and 10.0 .

Fig. 6. The temperature dependence of the condensate, normalized to its zero temperature value. The approximation $\bar{E}_\beta(p) = m_\beta^*$ has been used.

Fig. 7. The temperature dependence of the dynamically generated quark mass is given as a function of the scaled temperature T/m^* .

Fig. 8. As in Fig. 5, with the momentum dependent ansatz $\bar{E}_\beta^2(p) = m_\beta^{*2} + p^2$.

Fig. 9. As in Fig. 6, with the momentum dependent ansatz $\bar{E}_\beta^2(p) = m_\beta^{*2} + p^2$.

Fig. 10. The condensate, shown for two arbitrary choices of the dynamically generated masses $m^* = 200\text{MeV}$ and $m^* = 300\text{MeV}$. The upper curves in each case correspond to the momentum independent ansatz $\bar{E}_\beta(p) = m_\beta^*$, while the lower correspond in each case to the dispersion ansatz $\bar{E}_\beta^2(p) = p^2 + m_\beta^{*2}$.

Fig. 11. The current quark masses, shown for two arbitrary choices of the dynamically generated masses $m^* = 200\text{MeV}$ and $m^* = 300\text{MeV}$. The upper curves in each case correspond to the momentum independent ansatz $\bar{E}_\beta(p) = m_\beta^*$, while the lower correspond to the dispersion ansatz $\bar{E}_\beta^2(p) = p^2 + m_\beta^{*2}$.

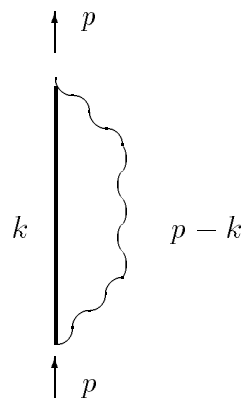


Figure 1

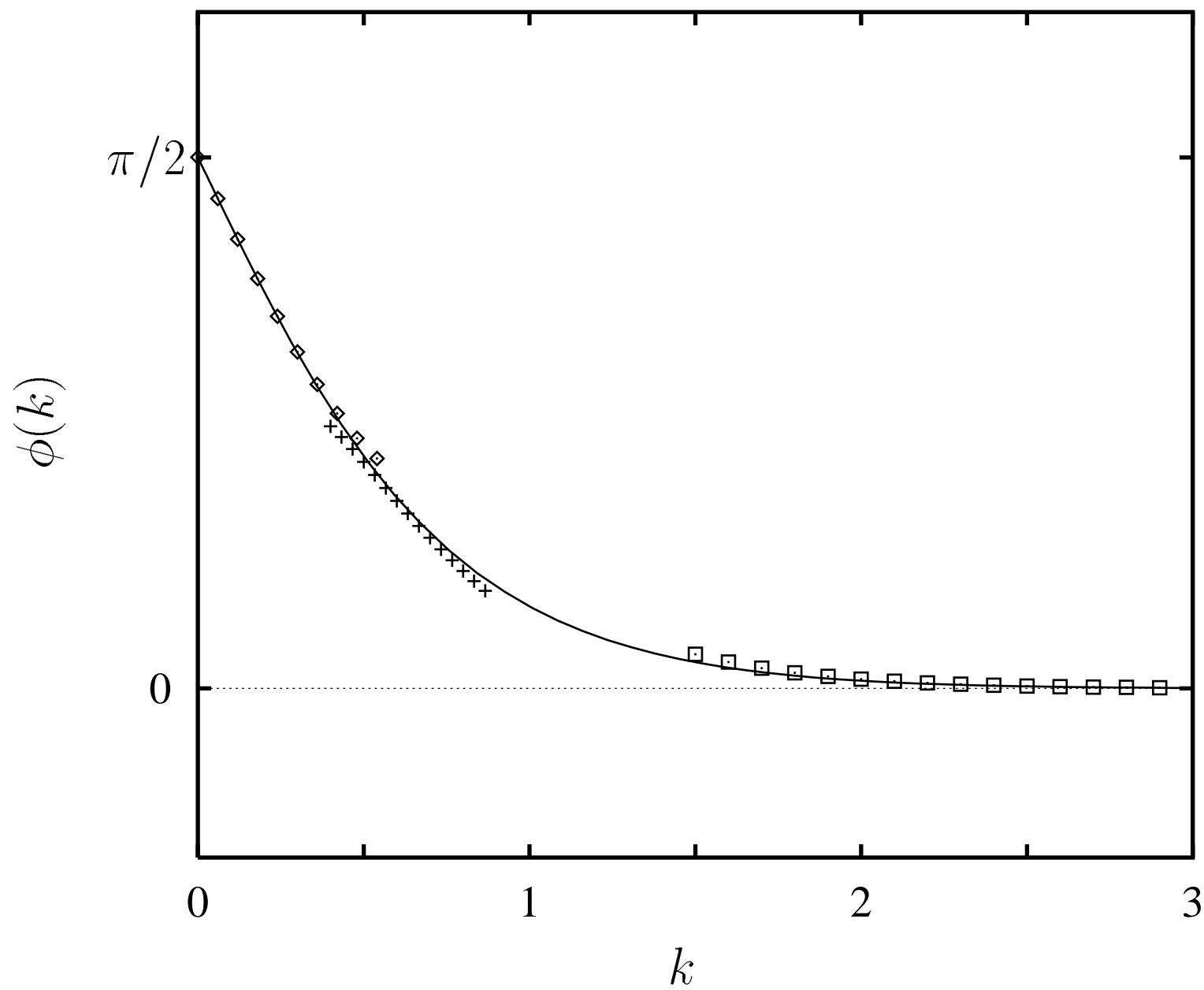


Figure 2

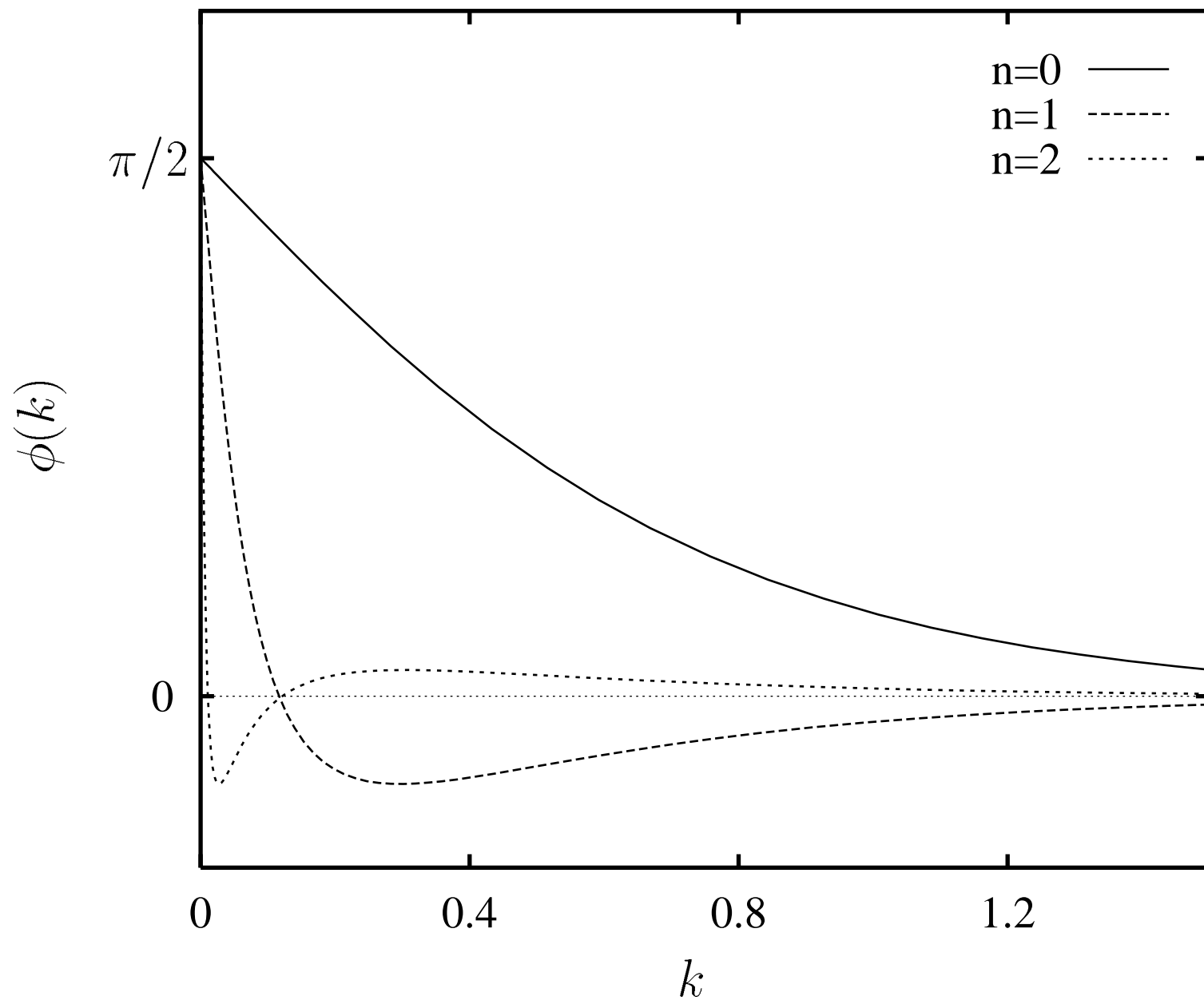


Figure 3

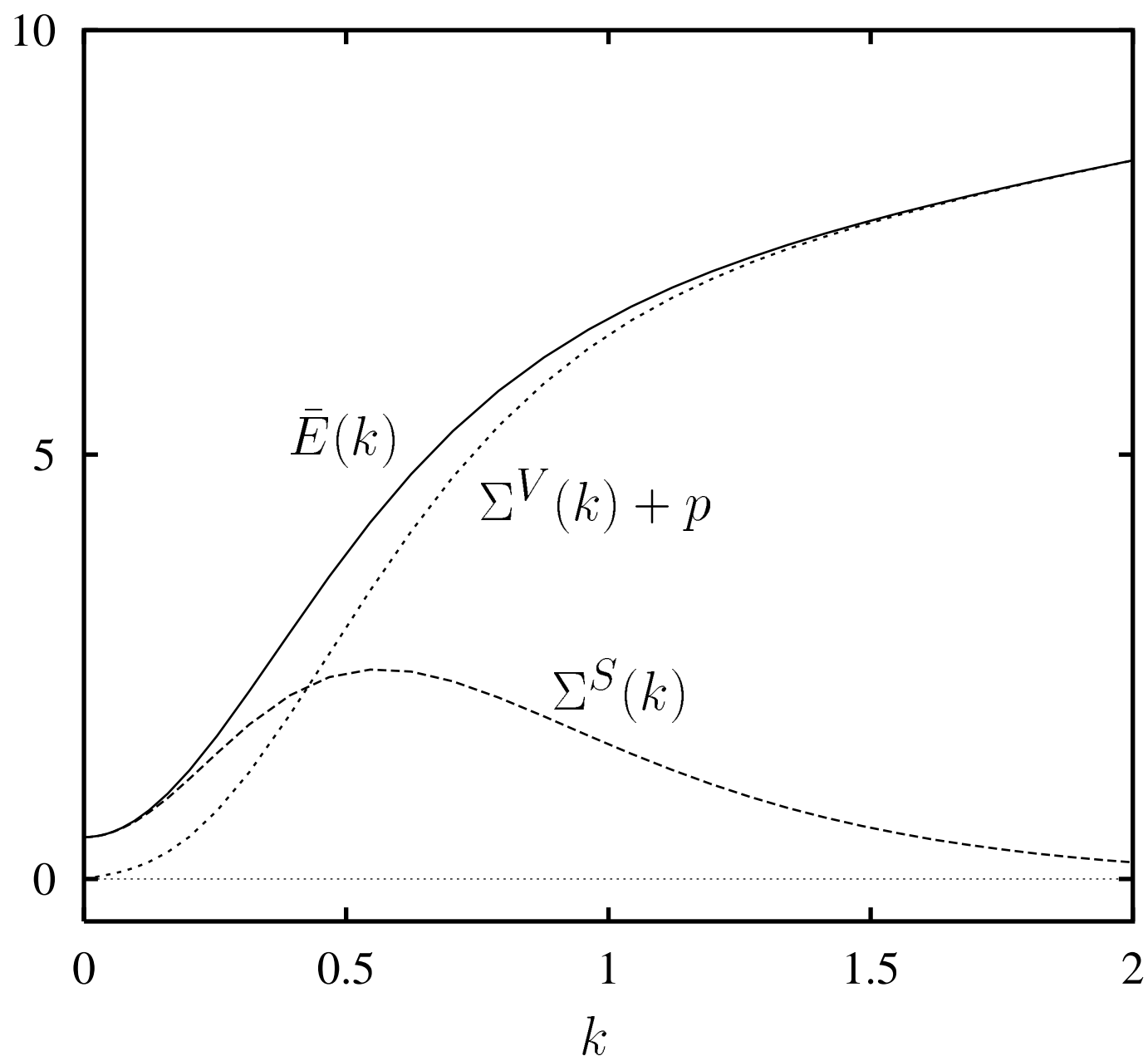


Figure 4

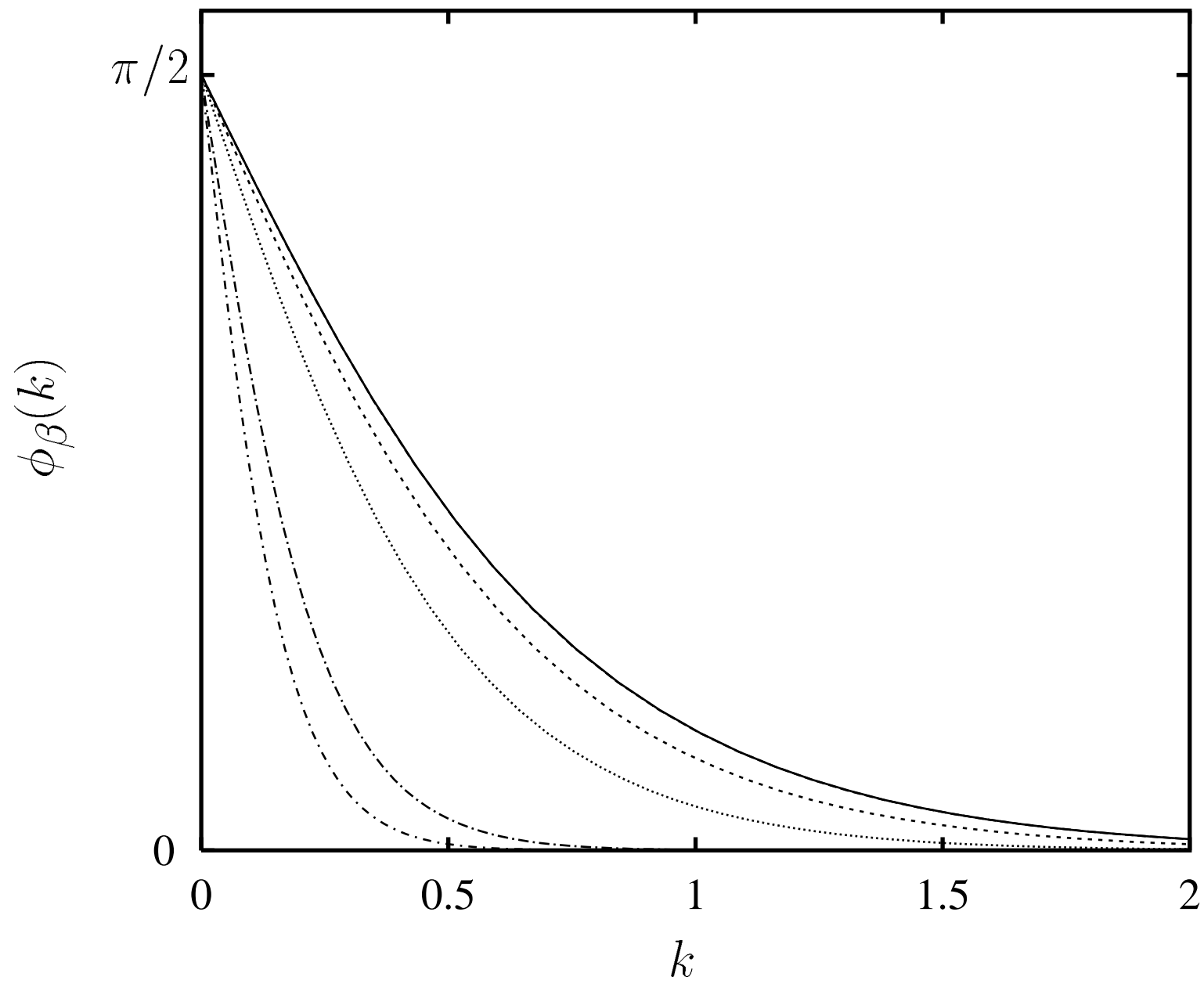


Figure 5

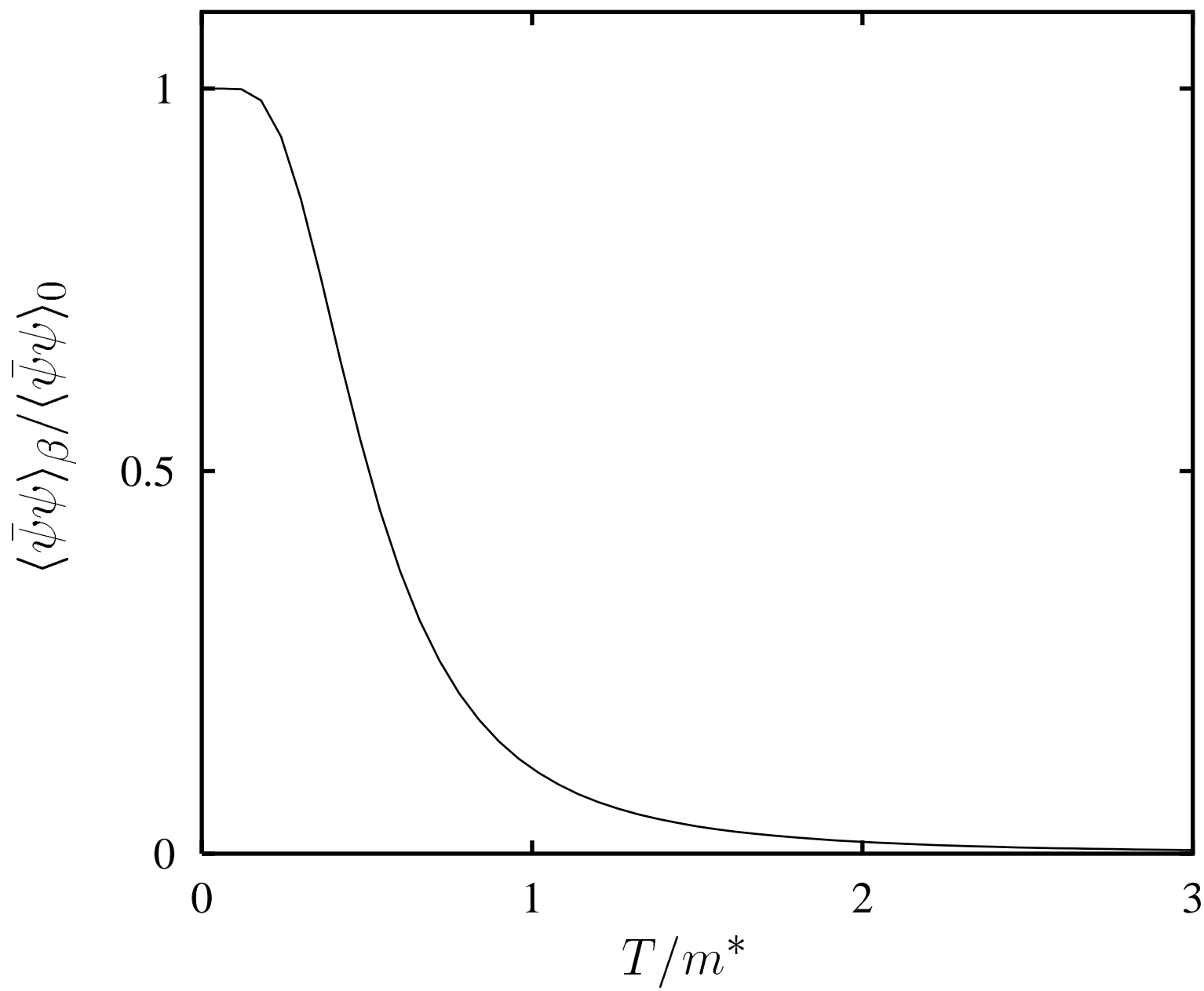


Figure 6

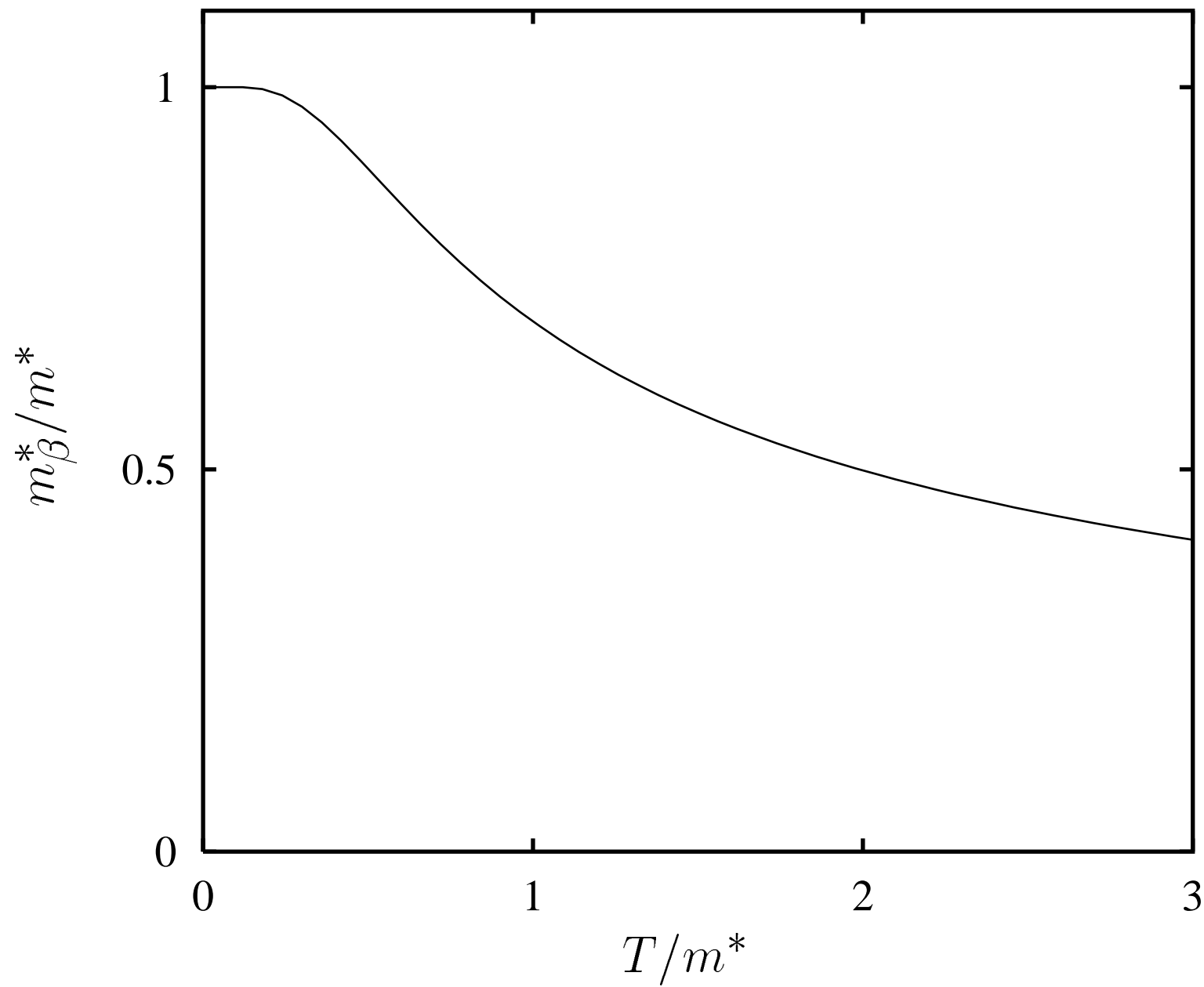


Figure 7

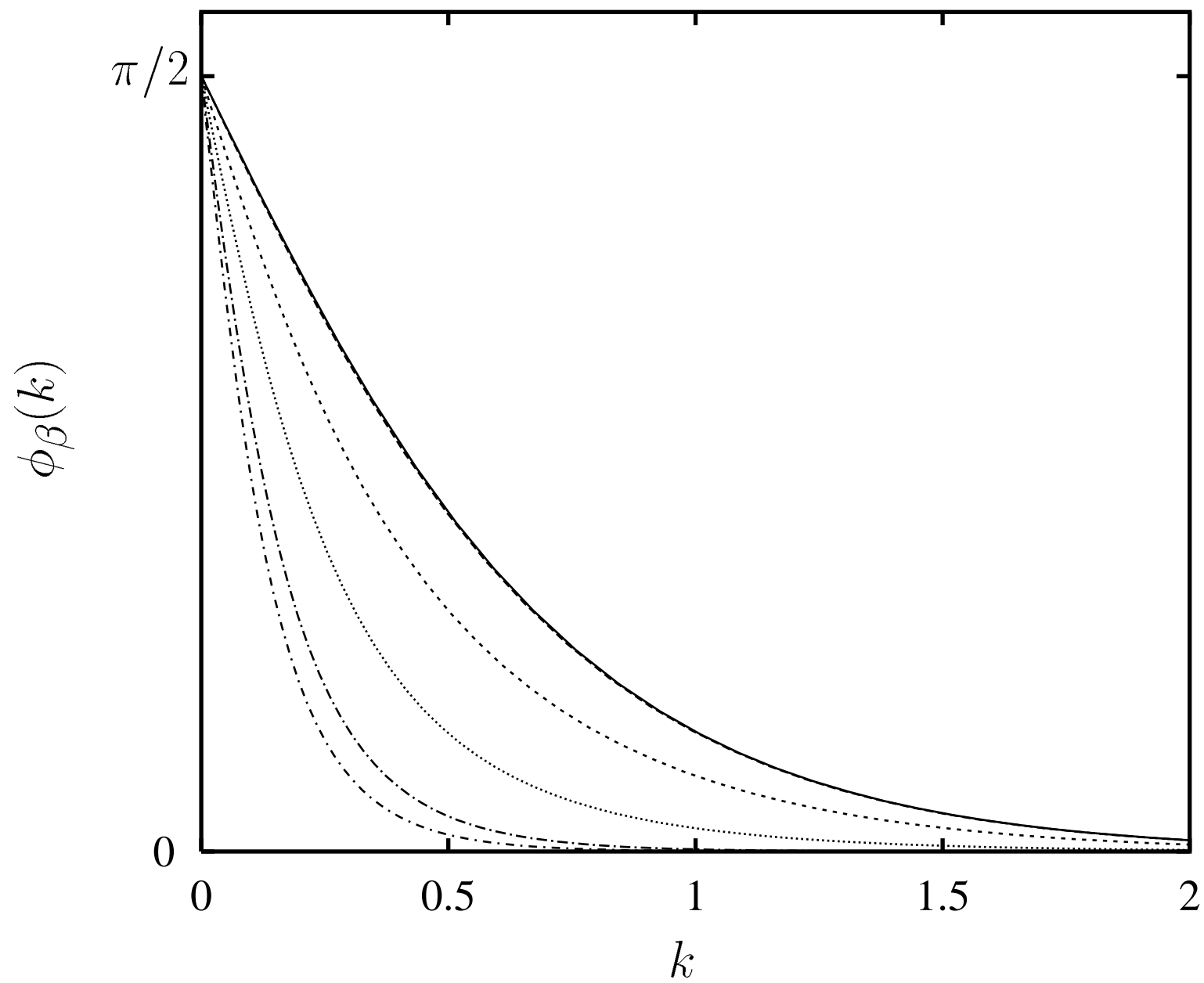


Figure 8

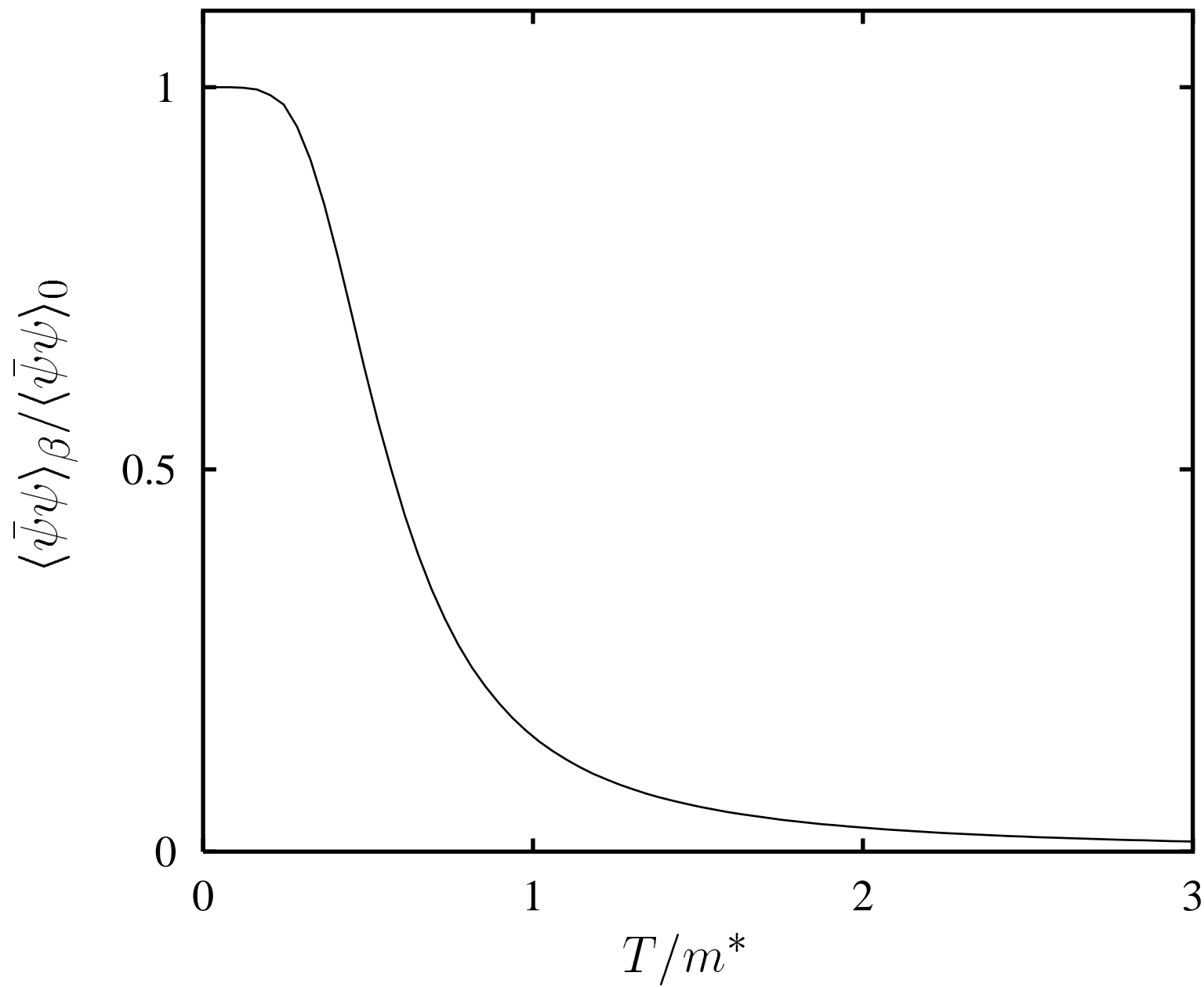


Figure 9

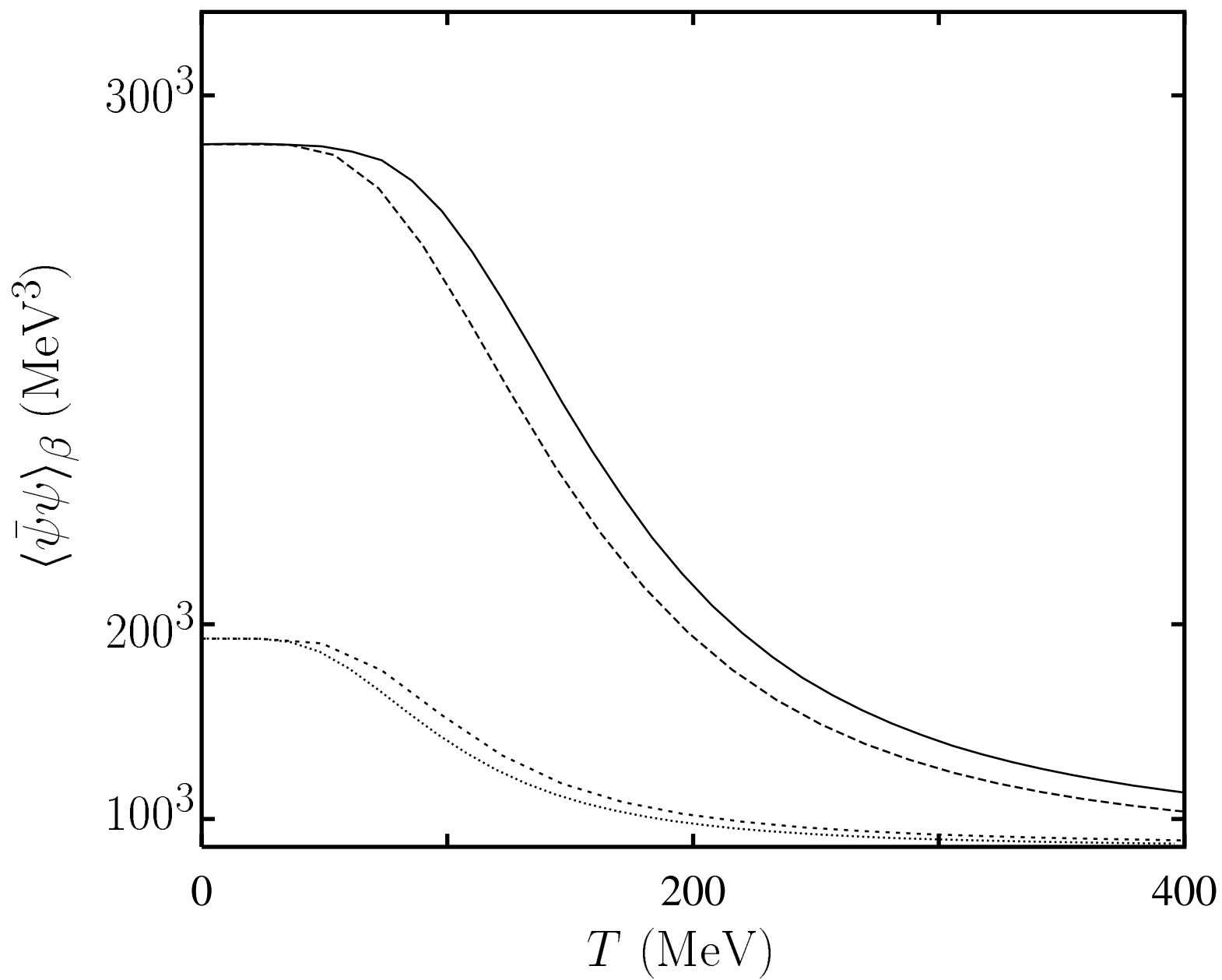


Figure 10

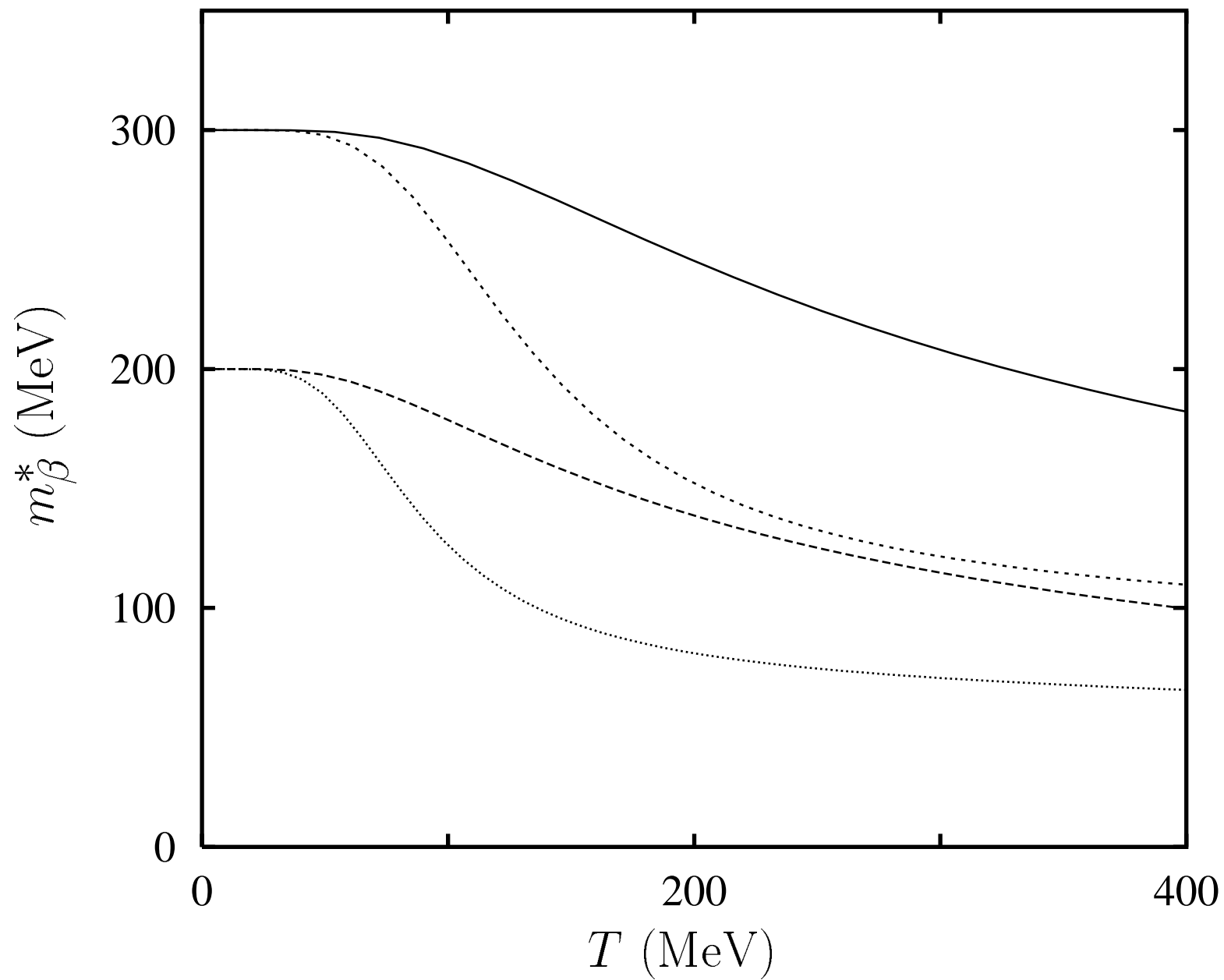


Figure 11